Key Engineering Materials
ISSN: 1662-9795, Vol. 1050, pp 113-122
doi:10.4028/p-Y3cBRq

Submitted: 2026-01-19
Revised: 2026-02-21
Accepted: 2026-02-21
Online: 2026-04-16

Robust and Feature-Aware Arbritary Lagrangian-Eulerian Method for Material Forming Applications

Garcia C. Jesus O.[1,a*], Alves Z. José R.[1,b], Ripert Ugo[1,c], Beraudo Christine[1,d]

[1]Transvalor S.A. E-Golf Park, 06410 Biot, France

[a]jesus.garcia@transvalor.com, [b]jose.alves@trasvalor.com, [c]ugo.ripert@transvalor.com, [d]christine.beraudo@transvalor.com

Keywords: ALE Method, Material Forming, Mesh Adaptation, FSW.

Abstract. Accurate simulation of material forming requires managing severe mesh distortions to preserve the geometry of the workpiece. Classical Lagrangian descriptions often become computationally expensive under such conditions. The Arbitrary Lagrangian-Eulerian (ALE) method offers a robust alternative by combining the strengths of Lagrangian and Eulerian descriptions, thereby improving computational efficiency and numerical stability. However, a major challenge remains in accurately handling free surfaces to maintain the geometric fidelity of the workpiece. This work introduces a new ALE-based approach to address this limitation. An analytical case as well as a Friction Stir Welding (FSW) case will be presented to demonstrate its effectiveness.

Introduction

In continuum mechanics, the description of motion requires specifying the reference with respect to which the body is observed. To this end, it is important to distinguish between the different configurations that can be associated with the body.
Three configurations are commonly considered:

- Material (reference) configuration (R_{x^*}): Represents the body in its original, undeformed state; each particle is labeled by its reference coordinate (x^*).
- Spatial (current) configuration (R_x): Represents the body in its current, deformed state; positions of material points are given by (x).
- Referential (mesh) configuration (R_χ): Represents the computational mesh; nodes at (χ) can move independently of the material.

These configurations provide the geometric framework for expressing the Lagrangian, Eulerian, and Arbitrary Lagrangian–Eulerian (ALE) descriptions of motion respectively.

Lagrangian description: In this approach, each mesh node moves with the material particle to which it is permanently attached. Consequently, the mesh velocity ($\vec{v}_{mesh}$) coincides with the material velocity ($\vec{v}_{mat}$), which is used to update the particle positions as:

$$\vec{v}_{mesh} = \vec{v}_{mat}(x^*, t) = \left.\frac{\partial x}{\partial t}\right|_{x^*} \tag{1}$$

In this description, the boundaries of the domain are naturally tracked by the mesh. Fig. 1a illustrates the evolution of a Lagrangian mesh M_{LAG} over a time step Δt. The Lagrangian description is particularly well suited for materials with history-dependent constitutive laws and is therefore widely used in structural and solid mechanics. However, it becomes challenging in the presence of large deformations, as severe mesh distortions may occur, often requiring frequent and complex remeshing procedures.

Eulerian description: In contrast to the Lagrangian description, the Eulerian approach is less affected by mesh distortion problems, as the mesh does not deform with the material. In this approach, the computational mesh remains fixed in space, while the material domain moves through it. The

material velocity ($\vec{v}_{mat}$) is therefore expressed with respect to the fixed mesh and does not reference the initial material coordinates x^*:

$$\vec{v}_{mesh} = 0 \; ; \; \vec{v}_{mat} = \vec{v}_{mat}(x,t) \tag{2}$$

This description enables the simulation of problems involving large deformations without mesh degradation. However, it introduces convective effects due to the relative motion between the material and the mesh. While the Eulerian approach is widely used in fluid dynamics, it presents challenges when applied to solid mechanics, particularly in tracking deformable free surfaces and material interfaces in unconfined flows. As illustrated in the Fig. 1b, the boundaries of the continuum do not necessarily coincide with the Eulerian mesh M_{EUL}.

ALE description: The ALE approach combines key features of both the Lagrangian and Eulerian descriptions. Neither the material configuration R_{x^*} nor the spatial configuration R_x is taken as the sole reference. Mesh nodes may move with the material, as in a classical Lagrangian description; remain fixed, as in a Eulerian approach; or move arbitrarily, allowing for continuous rezoning of the mesh. The mesh velocity ($\vec{v}_{mesh}$) is therefore defined by:

$$\vec{v}_{mesh} = \left.\frac{\partial x}{\partial t}\right|_{\chi} \tag{3}$$

This flexibility enables the ALE method to accommodate large distortions while still accurately tracking domain boundaries. However, it also inherits computational challenges from both Lagrangian and Eulerian descriptions, particularly in the treatment of convective terms and in the implementation of robust mesh-update procedures. Fig. 1c illustrates the evolution of an ALE mesh M_{ALE} over a time step Δt.

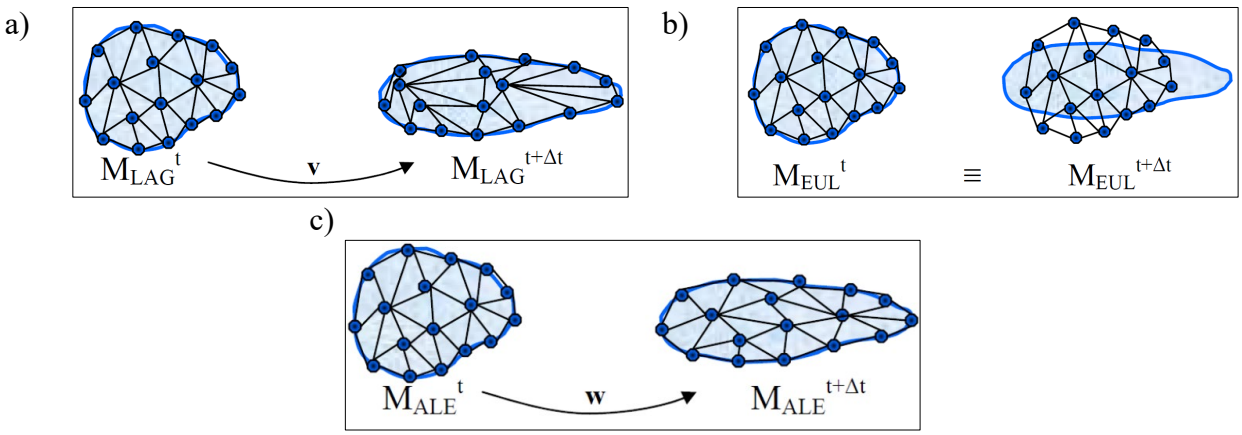

Fig. 1. a) Lagrangian description, b) Eulerian description, c) ALE description [2]

Convective transport: After mesh regularization, field variables must be transported from the original mesh to the updated one. This is commonly achieved using a convective transport approach. In the ALE description, since the reference domain differs from the material domain, the time derivative of a field $\left(\frac{d\zeta}{dt}\right)$ involves both a time grid derivative $\left(\frac{d_g\zeta}{dt}\right)$ and a convective term $\left(\vec{c}\cdot\vec{\nabla}\zeta\right)$:

$$\frac{d\zeta}{dt} = \frac{d_g\zeta}{dt} + \vec{c}\cdot\vec{\nabla}\zeta \tag{4}$$

Where $\vec{c}$ is the convective velocity and it is defined as.

$$\vec{c} = \vec{v}_{mat} - \vec{v}_{mesh} \tag{5}$$

The field update in the ALE formulation is then expressed as:

$$\zeta_{ALE}^{t+\Delta t} = \zeta_{ref}^{t} + \int_{\Delta t} \frac{d_g \zeta}{dt} \tag{6}$$

With

$$\frac{d_g \zeta}{dt} = \frac{d\zeta}{dt} - \vec{c} \cdot \vec{\nabla}\zeta \tag{7}$$

Linearizing the above expression and using a finite difference scheme, the updated field can be written as:

$$\zeta_{ALE}^{t+\Delta t} = \zeta_{LAG}^{t+\Delta t} - \vec{\nabla}\zeta_{LAG}^{t+\Delta t} \cdot \vec{c}\, \Delta t \tag{8}$$

Arbitrary Lagrangian–Eulerian Method

Two main ALE strategies are commonly used:

- A fully coupled approach, which directly solves convection–diffusion equations.
- An uncoupled approach, which solves the global system's resolution separated for convection.

In this work, the uncoupled approach, better suited for Lagrangian-based finite element codes, is adopted. It consists of computing a mesh velocity to regularize the mesh, followed by a remapping step between the original and the adapted meshes. This strategy allows the global mechanical resolution to be decoupled from mesh adaptation [1,2].

Mesh Velocity Computation: The ALE method can also be viewed as an r-adaptation technique, where mesh connectivity is preserved and only node positions are updated. This makes it significantly faster than full remeshing approaches.

Mesh velocity can be computed using either:

- Explicit methods, such as centering techniques that average neighboring node information.
- Implicit methods, which minimize quantities such as the gradient of mesh velocity.

In this work, an implicit approach is adopted, allowing the mesh velocity to be computed globally across the entire mesh. The mesh displacement ($\vec{u}$) is computed first, from which the mesh velocity is subsequently obtained.

Mesh displacements are computed using a weak formulation of linear elasticity expressed in terms of the displacement field. Dirichlet boundary conditions are applied in regions defined as purely Eulerian within the mesh.

$$\begin{aligned} -\vec{\nabla} \cdot \sigma(\vec{u}) &= \vec{f} \qquad in \quad \Omega \\ \vec{u} &= 0 \qquad on \ \partial\Omega_D \end{aligned} \tag{9}$$

Where σ is the Cauchy stress tensor and $\vec{f}$ is an external load applied to Ω.

Transport: To handle the remapping step, advantages and limitations of the convective method, expressed in equation (8), are taken into account. The main difficulty of this method arises when computing the gradient ($\nabla\xi^{t+\triangle t}$).

A common approach involves identifying, for each point, the corresponding upstream element based on the mesh velocity at the current time step. This is typically performed using an upwind method (Fig. 2a), in which the search direction is determined by the convective velocity. However, such

element-tracking procedures can be computationally expensive and challenging to implement efficiently in a distributed parallel framework.
An alternative and robust strategy consists of enriching the fields by projecting them from Gauss points to nodes and then back to super-convergent integration points (Gauss points), where the gradient can subsequently be computed elementwise. While this approach simplifies the search process, it introduces significant numerical diffusion in the transported fields [2].

To overcome these issues, the present work proposes a strategy that combines the strengths of different approaches to preserve both accuracy and computational efficiency. First, the field ξ is evaluated on the current mesh configuration at the Gauss-points level and then recovered on the nodes, thereby constructing a continuous P_1 field, this P_1 field is subsequently re-interpolated at the P_1 Gauss points of the elements.
At this stage, a continuous field distribution is available and can be trasported to the P_1 Gauss points of the updated mesh. This is achieved by localizing each Gauss point of the new mesh within the previous mesh using a logarithmic search algorithm (octrees are employed in this work), followed by interpolation using the local shape functions of the reference element [3] (see Fig. 2b).
In other words, directional searches are replaced by a straightforward point-wise localization procedure, since the direction of convection is already embedded in the previously enriched field.

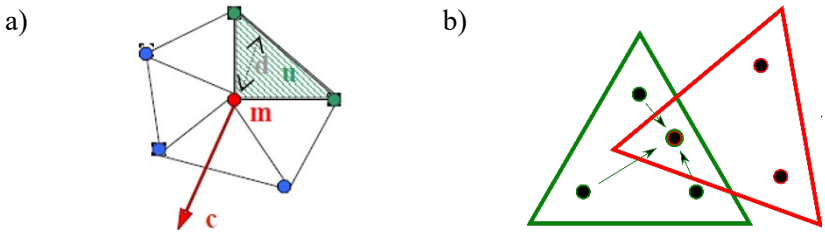

Fig. 2. a) upwind element [2], b) interpolation strategy, current element (green), updated element (red)

To prove the pertinence of this choice an analytical test is performed, which is shown in Fig. 3, this demonstrates successful convection of the analytical field. Although some numerical diffusion is observed, the initial field is still well preserved. Differences between fields stored at nodes and at Gauss points are also visible, reflecting the richer spatial sampling provided by using four Gauss points per element, which enhances transport accuracy between both meshes.

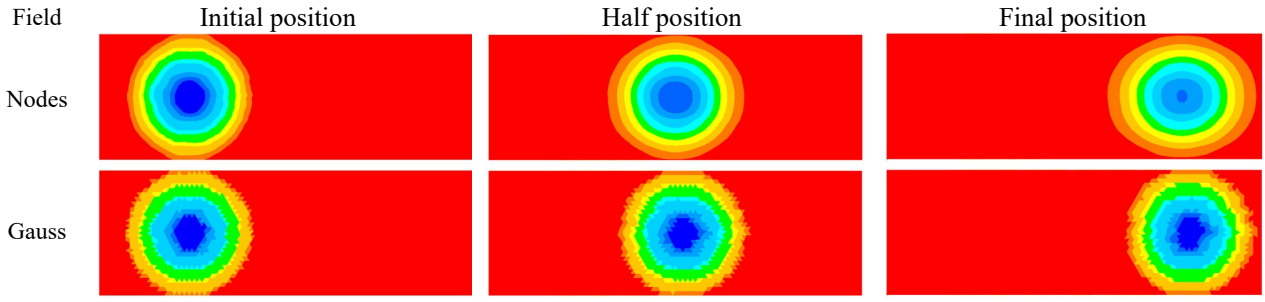

Fig. 3. Transport test using the interpolation strategy for nodes and elements stored fields

Dealing with Free Surfaces:
One of the main challenges in ALE methods is the accurate treatment of free surfaces, which can otherwise lead to loss of volume and distortion of the geometry [4-7]. To address this issue, a new and robust approach has been implemented.

Special attention is given to surface elements in order to accurately preserve the geometric shape. This requires proper identification of the local geometric characteristics of each surface node, which is determined by analyzing the patch of element faces surrounding the node. This analysis provides

information about whether the node belongs to a planar or curved surface, an edge, or a corner. To achieve this, a voting normals technique is employed [8]. The resulting normals characterize the local geometry: one normal indicates a node located on a planar or curved surface, two normals identify an edge node, and three normals correspond to a corner node, as illustrated in Fig. 4.

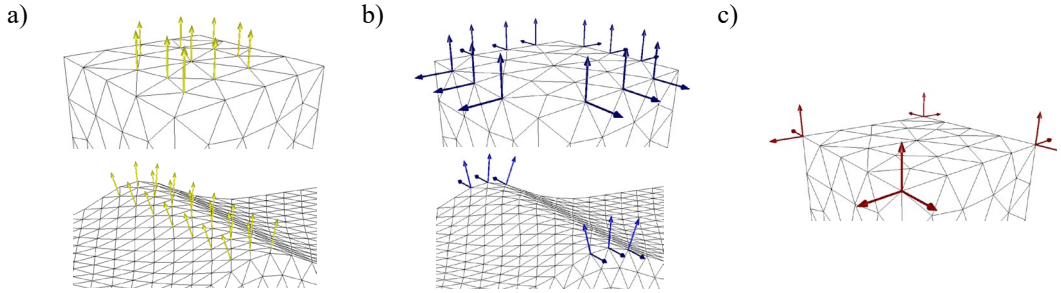

Fig. 4. Voting normals: a) 1 normal: continuous surface, b) 2 normals: edge feature between two surfaces, c) 3 normals: corner.

Once the surface normals are identified, they are used to construct a transformation matrix at each surface node. This matrix is then applied locally to rotate the stiffness matrix of the linear elasticity problem. This formulation preserves the geometric shape by enforcing displacement constraints consistent with the nature of the free surface. Because the transformation matrix is built from the oriented normals, each of the previously identified cases must be treated separately.

For a node associated with a single normal (surface node), displacement is constrained in the normal direction by imposing a Dirichlet boundary condition in that direction, while displacements along the two tangential directions remain allowed. For an edge node, displacement is permitted only along the tangential direction, and the other two directions are constrained. For a corner node, displacements are constrained in all three directions. These cases are illustrated in Fig. 5.

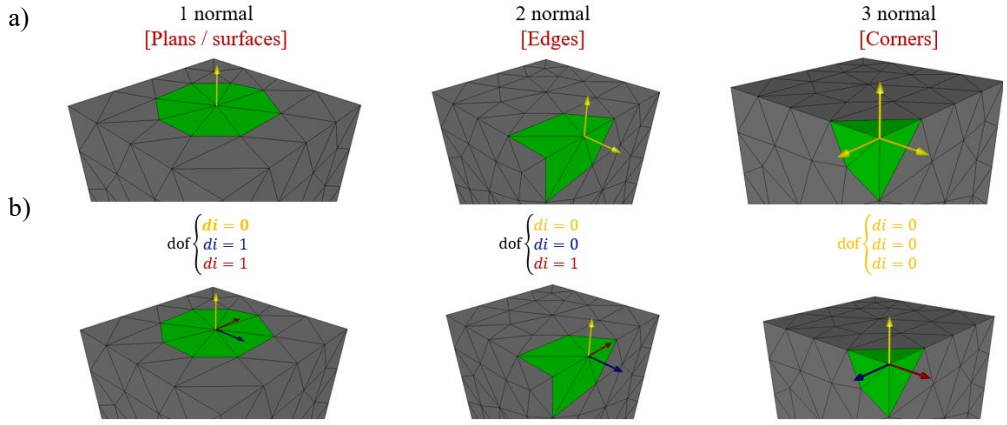

Fig. 5. a) Normals on a mesh, b) Degrees of freedom applied in each direction according to the number of normals

Analytical case

To validate the proposed method, an analytical test case was performed. The objective is to assess the ability of the approach to preserve the geometry of the workpiece while performing mesh regularization.

In this test, the mesh is deformed according to the analytical function, as illustrated in Fig. 6a. Both ends of the geometry move to the right, while a wave is generated in the central region. The goal is to let the wave propagate while keeping the extremities fixed, allowing the ALE approach to handle

mesh regularization in the remaining part of the geometry. The corresponding boundary conditions are applied as shown in Fig. 6b.

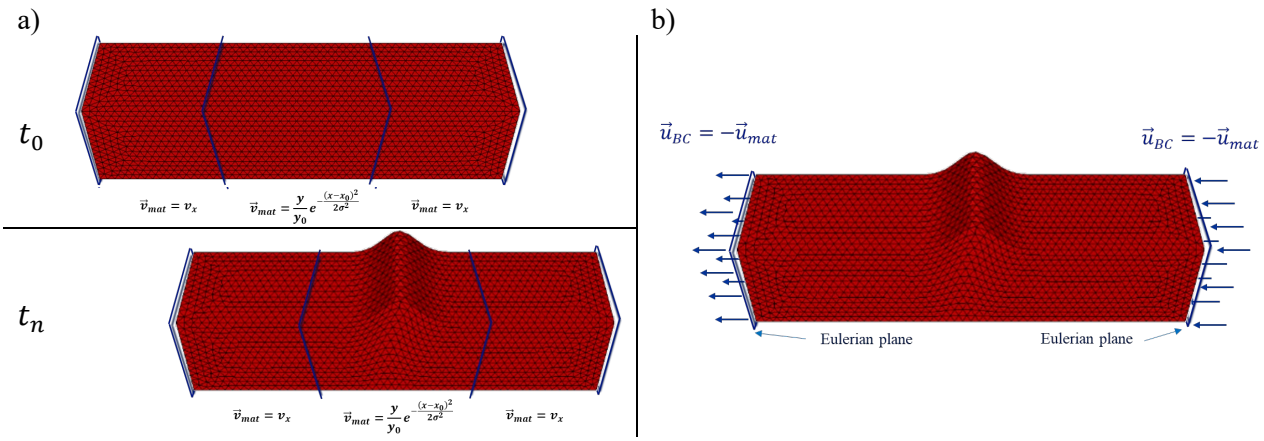

Fig. 6. Analytical case: a) analytical function at the initial (t_0) and at time step n (t_n), b) Boundary conditions applied in then ALE approach

The proposed methodology was applied, and the resulting displacement field exhibits very promising behavior. In particular, the computed displacements correctly follow the evolution of the free surfaces, as shown in Fig. 7.

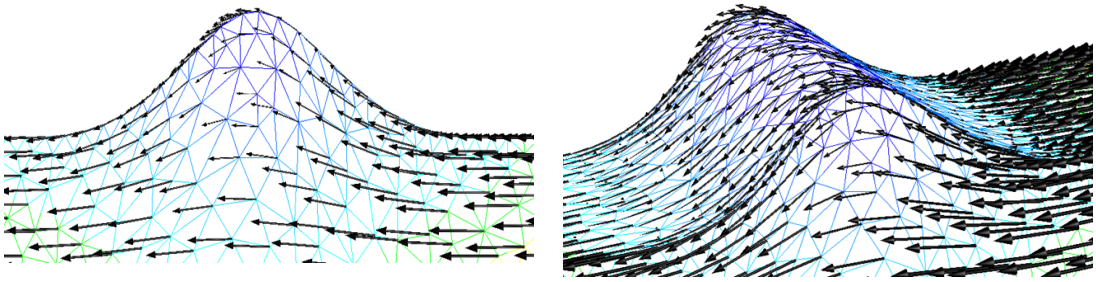

Fig. 7. ALE displacement field on the mesh.

A comparison between the Lagrangian solution (blue) and the ALE solution (red), illustrated in Fig. 8, demonstrates excellent agreement at this stage of the simulation. The wave shape is well preserved in the ALE mesh and closely matches the Lagrangian solution. This confirms the effectiveness of the proposed method in preserving free surfaces while maintaining mesh quality and delaying the need for remeshing.

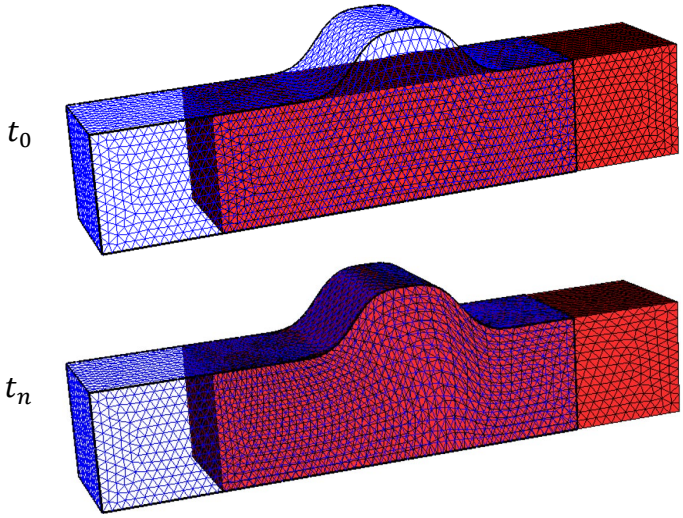

Fig. 8. Comparison of the Lagrangian (blue) and ALE (red) mesh configurations at the initial (t_0) and at time step n (t_n)

Application to the Friction Stir Welding (FSW) Process

Friction Stir Welding (FSW) converts mechanical energy into heat and material deformation in order to create a weld. In this process, the parent material does not melt; joining occurs in the solid state, as illustrated in Fig. 10a, thereby avoiding potential metallurgical issues such as porosity, cracking, or undesirable microstructural changes

The test case is taken from Fourment and Guerdouxs work [9].The FSW process is modeled using a single-plate configuration, without explicitly representing the interface between the welded plates (Fig. 9b). The tool is assumed to be stationary (Fig. 9c), while motion is imposed on the plate, as shown in Fig. 10a.

In this model, motion is imposed on the plate, making it the only moving component. As in the analytical case, the objective of the ALE approach is to prevent the rigid translation of the workpiece to the left, thereby keeping the geometry fixed during the simulation. To achieve this, appropriate boundary conditions are applied (see Fig. 10b), consisting of a displacement imposed in the direction opposite to that of the kinematic model. This ensures zero net displacement of the geometry, while the ALE formulation accommodates the relative motion within the remaining part of the mesh.

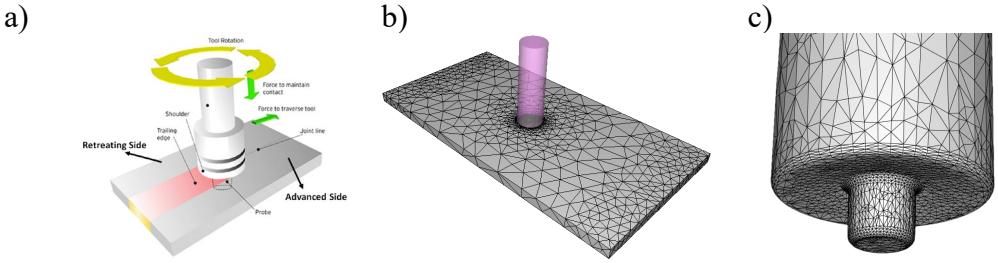

Fig. 9 a) FSW scheme process, b) simulated plate and tool, c) tool design.

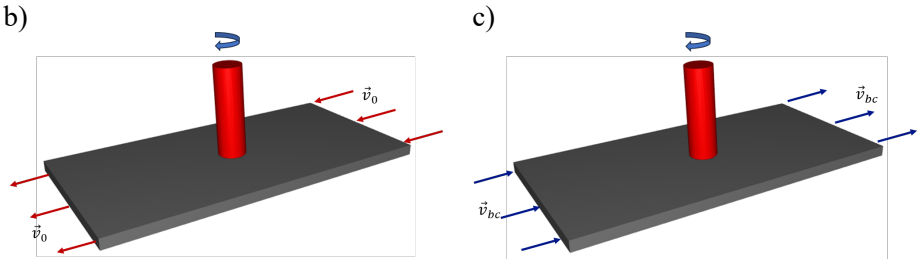

Fig. 9 a) model's kinematics, b) boundary conditions for ALE

The proposed ALE approach is compared with a classical Lagrangian formulation and with a previously developed ALE method. Results are displayed in Fig. 11, the former ALE approach exhibits excessive mesh smoothing, leading to poor preservation of free surfaces and the loss of the trailing edge during the welding process. In contrast, the proposed ALE method accurately preserves the workpiece geometry, yielding results that closely match the Lagrangian solution.

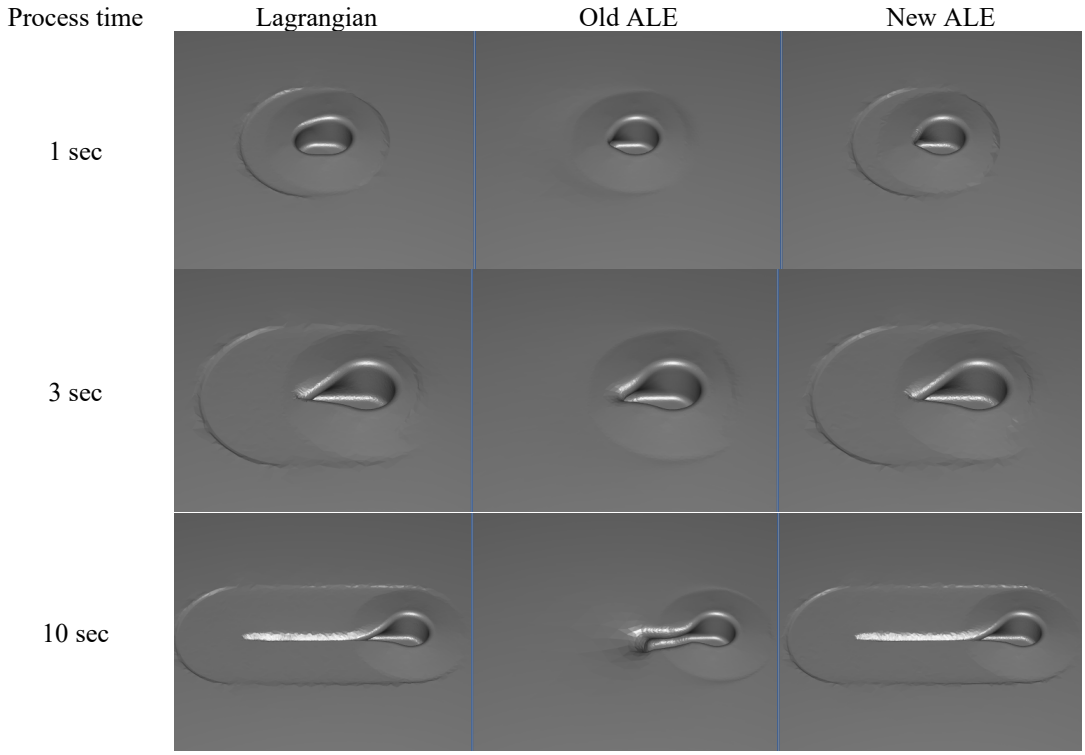

Fig. 10 Comparation of different methods at 1, 3 and 10 seconds of process simulation

Fig. 12 displays a direct comparison between the Lagrangian mesh (mesh lines) and the proposed ALE mesh (in magenta) shows an excellent geometric agreement, with only a minor volume loss observed in the ALE case.

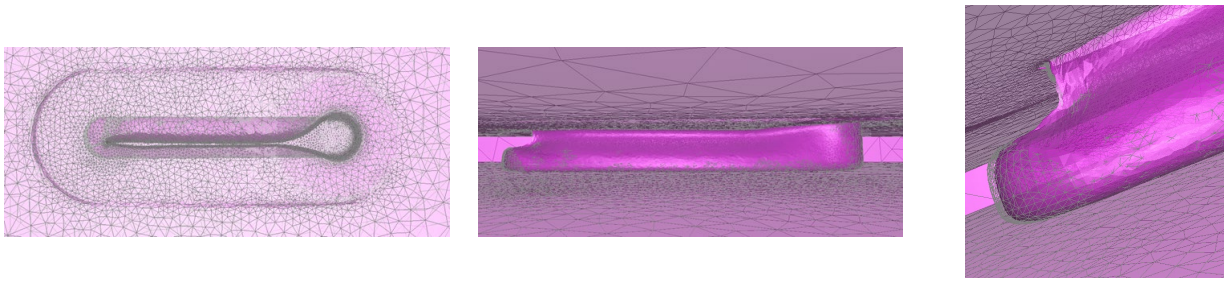

Fig. 11 Lagrangian (mesh lines) and ALE (in magenta) meshes comparison.

Additionally, temperature and equivalent strain fields results are also displayed in Fig. 13 and shown a very good agreement between the two simulations. Equivalent strain presents a small difference possible due to a small diffusion on the remapping procedure

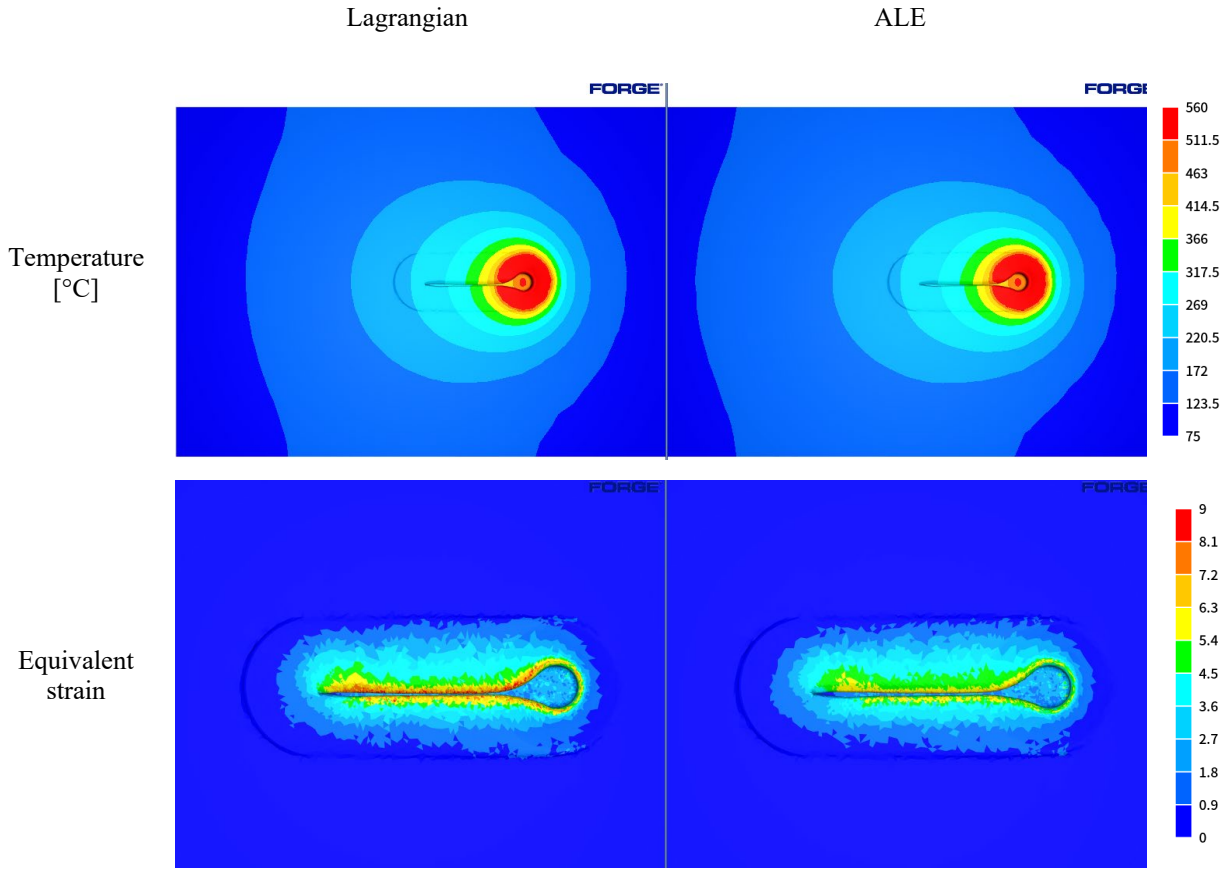

Fig. 12 Temperature and equivalent strain comparison

Summary

A new ALE method for material forming applications has been developed, featuring a robust strategy for preserving workpiece geometry based on voting normals and local matrix transformations at free-surface nodes. The method has demonstrated its effectiveness through both an analytical test case and an industrial-scale application involving Friction Stir Welding (FSW). In both cases, the proposed approach successfully preserves geometric integrity while maintaining good accuracy in the simulation results.

References

[1] M. Bellet and V. Fachinotti, "ALE method for solidification modelling," *Comput. Methods Appl. Mech. Eng.,* vol. 193, no. 39–41, pp. 4355–4381, 2004, doi: 10.1016/j.cma.2003.11.016.

[2] S. Guerdoux, "Numerical simulation of the friction stir welding process", Ph.D. dissertation, Ecole des Mines de Paris, France, 2007.

[3] H. Eldahshan, P.-O. Bouchard, J. Alves, E. Perchat, and D. Pino Munoz, "Phase field modeling of ductile fracture at large plastic strains using adaptive isotropic remeshing," *Comput. Mech.*, vol. 67, pp. 763–783, 2021, doi: 10.1007/s00466-020-01962-7

[4] S. Philippe, "Development of an ALE formulation for 3D rolling simulation" Ph.D. dissertation, Ecole National Supérieur des Mines de Paris, France, 2009.

[5] S. Philippe, L. Fourment, and P. Montmitonnet, "Application of the arbitrary Lagrangian–Eulerian formulation to the numerical simulation of stationary forming processes with dominant tangential material motion," in *Proc. 12th Int. Conf. Metal Forming*, Cracow, Poland, Sep. 2008, pp. 571–578.

[6] M. Hachani, “Improved contact treatment for metal forming processes with reduced contact area”, Ph.D. dissertation, Ecole National Supérieur des Mines de Paris, France, 2011.

[7] S. Gastebois, “Numerical simulation of FSW welding using an ALE formulation”, Ph.D. dissertation, Ecole National Supérieur des Mines de Paris, France, 2015.

[8] G. G. Medioni, M. Lee, and C. Tang, *A Computational Framework for Segmentation and Grouping*. Amsterdam, The Netherlands: Elsevier Science, 2000.

[9] L. Fourment and S. Guerdoux, “3D numerical simulation of the three stages of friction stir welding based on friction parameters calibration,” *Int. J. Mater. Form.,* vol. 1, suppl. 1, pp. 1287–1290, 2008, doi: 10.1007/s12289-008-0138-5.